

Simulated Epidemics in 3D Protein Structures to Detect Functional Properties

Mattia Miotto*,^{1,2} Lorenzo Di Rienzo*,¹ Pietro Corsi,³ Domenico Raimondo,⁴ and Edoardo Milanetti^{1,2}

¹*Department of Physics, Sapienza University of Rome, Rome, Italy*

²*Center for Life Nanoscience, Istituto Italiano di Tecnologia, Rome, Italy*

³*University "Roma Tre", Department of Science, Rome, Italy*

⁴*Department of Molecular Medicine, Sapienza University of Rome, Rome, Italy*

The outcome of an epidemic is closely related to the network of interactions between the individuals. Likewise, protein functions depend on the 3D arrangement of their residues and on the underlying energetic interaction network. Borrowing ideas from the theoretical framework that has been developed to address the spreading of real diseases, we study the diffusion of a fictitious epidemic inside the protein non-bonded interaction network. Our approach allowed to probe the overall stability and the capability to propagate information in the complex 3D-structures and proved to be very efficient in addressing different problems, from the assessment of thermal stability to the identification of allosteric sites.

Introduction

Proteins are large biomolecules responsible for the majority of live-sustaining tasks in cells. Their great versatility is due to the complex tridimensional structure they can acquire, that arises as a result of physical and chemical interactions among all its constituent amino acids. In particular, the global structure is uniquely defined once the sequence of amino acids composing the molecule is specified, with different sequences that can give, up to local rearrangements, the same overall 3D architecture.

The peculiar structural conformation each protein assumes is the result of a long evolutionary optimization. Proteins are adapted to carry on specific tasks, usually binding to other molecules while being embedded in a complex dynamical environment in the presence of both thermal and molecular noises. In this scenario what evolution does is to select sequences that allow proteins to exert their task more efficiently in the environment they live in while maintaining the same overall 3D architecture.

Understanding the rules that govern which features in the amino acid sequence can improve protein efficiency while preserving the biological function has both theoretical and practical implications. Many works investigated the role of different amino acids in the protein structure, folding, stability and dynamics [1]. In this respect, methods based on graph theory approaches have contributed considerably to the understanding of protein structural flexibility, their hierarchy of structures and in the identification of key residues [2–6]. All those findings demonstrated that a network-based analysis can be pivotal to shed light on the complex aspects relative to the organization of protein structures [7]. However, network approaches have often focused on a static description of the system while interesting properties, especially at the level of the single residue, are related to the dynamical behavior of the network [8].

Here, we combine a graph-based schematization of proteins together with an epidemic diffusion algorithm to study the overall stability and the capability to propa-

gate perturbations (or information) in their complex 3D-structures [9, 10].

In particular, our novel approach proved to be very efficient in characterizing protein thermal stability and in identifying allosteric sites of proteins, where trivial static network descriptors exhibit a lower efficiency.

Methods

A. Datasets

To investigate the capability of the diffusion protocol to grasp the essential feature of the protein structure and function, we defined four different datasets:

- A dataset of 32 pairs of homologous proteins with different thermal properties was manually collected from literature [11–14]. Experimentally determined structures were collected from the PDB [15] and filtered according to method (x-ray diffraction), resolution (below 3 Å), and percentage of missing residues (covering more than 95% of to the Uniprot [16] sequence). Proteins for which experimentally determined structures were only available in a bound state, i.e. in complex with either a ligand or an ion, were excluded. We will refer to this dataset as the Tm dataset (see Table I).
- A further "Enzyme dataset" was composed grouping all the enzymes present among the proteins of the Tm dataset. For each enzyme, we retrieved information about the residues forming the active site (see Table I), from the Enzyme Portal of EBI [17].
- From [18], we collected another dataset composed of proteins whose both active and allosteric sites are known. We named this dataset the Allosteric dataset.
- Finally, we took from [19] a fourth dataset composed by 2 apo structures of the HIV1 e HIV2 proteases together with 16 hole PDB structures (8 of

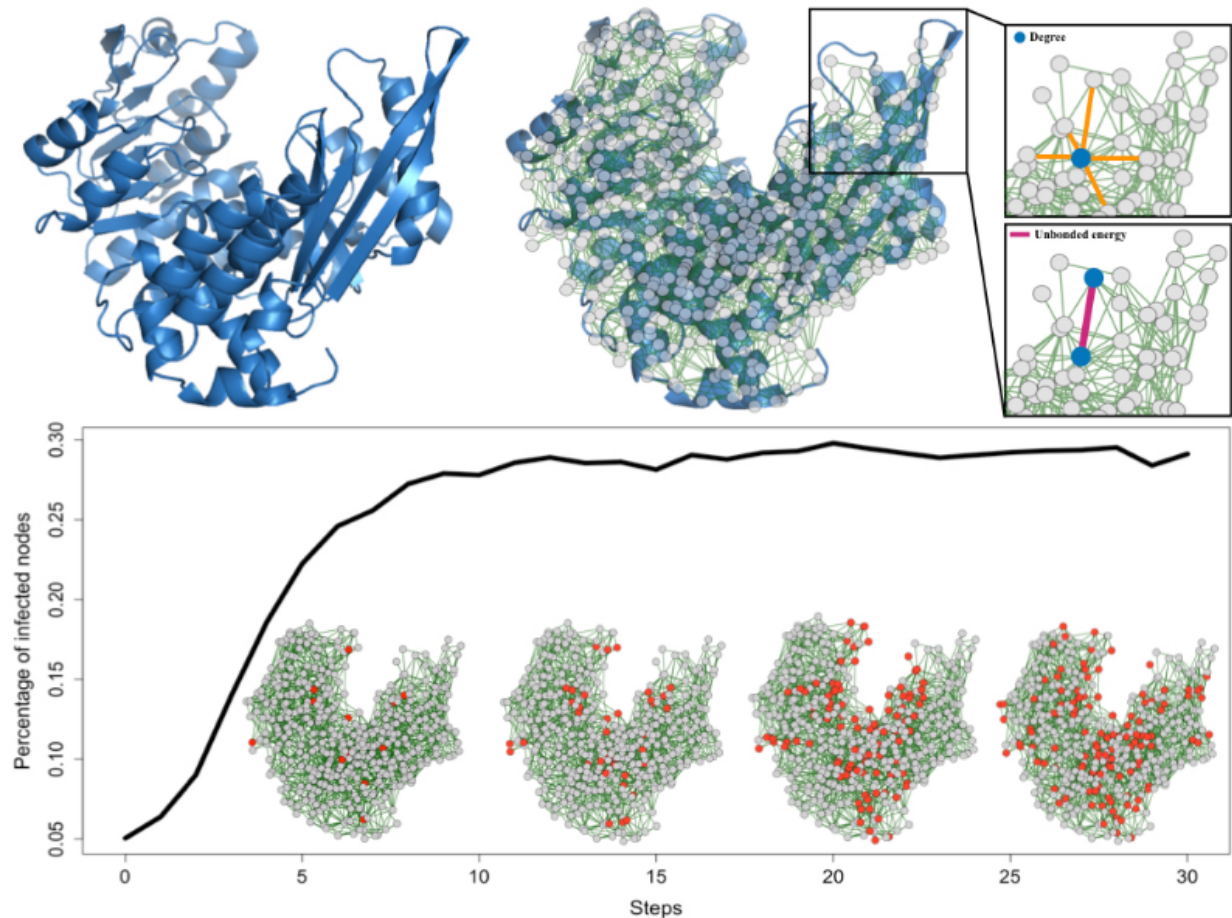


FIG. 1: Scheme of the diffusion procedure. **Top panel:** The transformation from a protein structure (left) to a Residue Interaction Network (RIN) (right). Protein residues are considered as nodes and the non-bonded energetic interactions between residues constitute the links between nodes. **Bottom panel:** The results of an epidemic diffusion over a protein RIN. We utilized interaction energy between residues and node degree as a proxy of infection and recover probability, respectively. Two parameters can be defined: the density of infected nodes at the stationary state, ρ^* , and the number of time steps necessary to reach the equilibrium value, t^* . The red nodes in the protein represent infected residues and their time evolution.

HIV1 and 8 of HIV2) being in complex with different ligands. HIV2 and HIV1 proteases display a very similar fold even if they have only about 50% of sequence similarity.

All protein structures were minimized using the standard NAMD [20] algorithm and the CHARMM force field [21] in vacuum. A 1 fs time step was used and structures were allowed to thermalize for 10000 time steps. This procedure aims at removing energetic clashes that may be present due to the crystallization procedure.

B. Network representation

Protein structures are represented as Residue Interaction Networks [22] (RINs in short), where each node represents a single amino acid aa_i . The nearest atomic distance between a given pair of residues aa_i and aa_j

is defined as D_{ij} . Two RIN nodes are linked together if $D_{ij} \leq 12 \text{ \AA}$ [20, 21]. Furthermore links are weighted by the sum of two energetic terms: Coulomb (C) and Lennard-Jones (LJ) potentials. The C contribution between two atoms, a_l and a_m , is calculated as:

$$E_{lm}^C = \frac{1}{4\pi\epsilon_0} \frac{q_l q_m}{r_{lm}} \quad (1)$$

where q_l and q_m are the partial charges for atoms a_l and a_m , as obtained from the CHARMM force-field: r_{lm} is the distance between the two atoms, and ϵ_0 is the vacuum permittivity. The Lennard-Jones potential is instead given by:

$$E_{lm}^{LJ} = \sqrt{\epsilon_l \epsilon_m} \left[\left(\frac{R_{min}^l + R_{min}^m}{r_{lm}} \right)^{12} - 2 \left(\frac{R_{min}^l + R_{min}^m}{r_{lm}} \right)^6 \right] \quad (2)$$

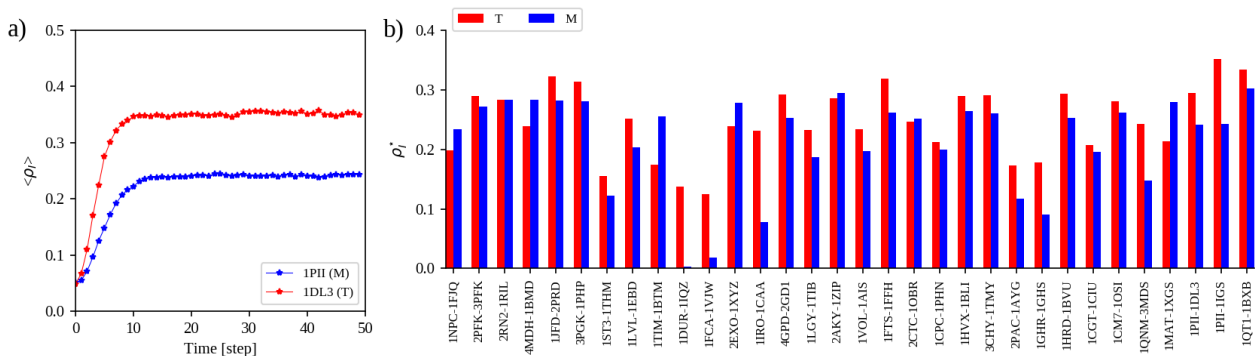


FIG. 2: **a)** Mean density of infected nodes as a function of time for an explicative homologous couple. **b)** Barplot representation of the density of infected node at the stationary state for the 32 mesostable (blue) and thermostable (red) proteins of the Tm dataset.

where ϵ_l and ϵ_m are the depths of the potential wells of atom l and m respectively, R_{min}^l and R_{min}^m are the distances at which the potentials reach their minima. Therefore, the weight of the link connecting residues aa_i and aa_j is calculated by summing the contribution of the single atom pairs as:

$$E_{ij} = \left[\sum_l^{N_i} \sum_m^{N_j} (E_{lm}^C + E_{lm}^{LJ}) \right] \quad (3)$$

where N_i and N_j are the numbers of atoms of the i -th and j -th residue respectively.

C. Diffusion model on the protein network

In the present work, we simulated an epidemic diffusion over the protein RINs. In particular, a SIS (susceptible-infected-susceptible) epidemic model is adopted where each node (i.e. residue) of the network can be found in two possible states: susceptible, S, (i.e unperturbed) or infected, I, (perturbed). Once infected, a node can transmit the infection to near neighbor nodes. Furthermore a residue can recover from the infection, returning to the susceptible state (meaning that it can be infected again). In this scenario, the probability of finding node i in an infected state is given by:

$$p_{t+1}^i = (1 - \delta^i)p_t^i + (1 - p_t^i) \sum_{a=1}^N \beta_{ij} p_t^j \quad (4)$$

where δ^i is the probability that in one-time step node i recovers from infection, while β_{ij} represents the probability that node i becomes infectious if node j is infected at time t . The model just described has been long studied in epidemic [23].

It has been found that, depending on the connectivity matrix architecture and the sets of $\{\delta_i\}$ and $\{\beta_{ij}\}$ parameters, the system can exhibit different behaviors. The infection, starting from some nodes, propagates in the whole network and reaches a stationary regime where a certain percentage p_i^* of nodes is constantly infected at each time, independently from the size and the identity of the initial set of infected nodes. Intuitively, $p_i^* = 0$ if the number of nodes that recover from the infection overcomes those that become infected. On the other hand, $p_i^* = 1$ when the infection is too aggressive. The nontrivial scenario ($0 \leq p_i^* \leq 1$) is achieved when the network architecture and the parameters allow having a balance between the number of nodes that become infected and the ones that recover.

For each RIN node we defined the recover probability, δ_i , and the infection probability between node i and j , β_{ij} . The former is defined as:

$$\delta_i = \frac{d_i}{(\max(d) + \epsilon)} \quad (5)$$

where d_i is the node degree and ϵ is a constant avoiding to have nodes that always recover. The infection probability is defined as

$$\beta_{ij} = \frac{|E_{ij}|}{\max(|E|) + \omega} \quad (6)$$

where E_{ij} is the interaction energy defined in Eq. 3 and again ω is a constant that avoids to have infection probability of one between certain nodes.

Once defined the infection and recover probabilities, it is possible to simulate the diffusion process, starting from a specific set of residues or by picking an initially random set, and looking at the mean density of infected residues over time:

$$\langle \rho_I(t) \rangle = \langle \frac{N_I(t)}{N_{tot}} \rangle \quad (7)$$

where $N_I(t)$ is the number of infected residue at time t , N_{tot} is the total number of protein residues and we indicated with $\langle . \rangle$ the mean over the M realizations of the diffusion process (presented results are obtained with $M=1000$).

Depending on the parameter set, as $t \rightarrow \infty$, $\langle \rho_I(t) \rangle$ can either go to zero, meaning that the network features do not favor diffusion, or alternatively $\langle \rho_I(t) \rangle$ can set on a certain mean level ρ^* (the single realization can give rise to oscillations that cancel out mediating over many realizations of the process). From the mean time evolution of ρ it is possible to define the transient time t^* as the first time at which $\rho(t^*) = \rho^* - \delta$, with $\delta \rightarrow 0$. Figure 1 provides a sketch of the process together with the descriptor definitions. In analyzing the results, R package stats [24] has been used. In particular, the clustering analysis performed on the HIV data made use of the HeatMap function, with Euclidean distance matrix given by the "dist" function and the "hclust" method for the clustering algorithm.

Results

D. Stationary epidemic behavior as a measure of protein thermal stability

Different thermal behaviors in homologous protein couples have long been studied and several features responsible for those differences were highlighted such as salt bridges, charged amino acids, etc. [25–31].

Most of the found biological ingredients responsible for increased thermal resistance are present in our network representation of the protein both in terms of network topology (structure) and link weights (energy). Here we exploit our epidemic-diffusion algorithm to assess the capability of the network to deal with temperature.

In particular, we compared the stationary state density of infected nodes between all the couples of Tm dataset. For each protein, the diffusion was simulated, starting each time from a randomly selected set of infected residues. In particular, 5% of the nodes are infected at $t = 0$. Each diffusion process was simulated for $T = 50$ steps.

In 75% (24 out of 32) of comparisons, thermophilic proteins acquire a higher density of infected nodes with respect to their mesophilic counterparts, when epidemic diffusion reach the equilibrium. This reflects both the overall higher connectivity and the higher energy of the links. In Figure 2a, we reported an example of the diffusion process in the IPII-1DL3 couple, where the different steady states are well visible.

E. Study of the transient phase: a local characterization

We then investigated the transient phase of the epidemic, and in particular the number of time steps necessary to reach the equilibrium. As said before, this time, t^* , varies depending on the set of infected initial nodes. If the epidemic starts from very central or energetically interconnected residues, it is very likely that the stationary state will be attained in a short time. Using this hypothesis, we simulate an epidemic originating from every single residue of all proteins in the dataset. In particular, for each amino acid, we selected its 2 closest neighbors in sequence (in order to avoid the fast extinction of the epidemic). In this way, we investigated which classes of amino acid are central in the protein network in order to achieve rapidly the equilibrium. To make the comparison between results coming from proteins of different sizes possible, it is necessary to normalize the results over each protein with the Z-score. Indeed the number of time steps necessary to reach the equilibrium in a very large protein will be necessarily larger than in a small protein, independently from the structural and energetic characteristics of the residues involved in spreading the epidemic. Therefore we normalize over every single protein with the z-score, so we can compare the results belonging to different proteins.

In particular, the z-score of the i -th residue is

$$Z_i = \frac{t_i^* - \langle t^* \rangle}{\sigma(t^*)} \quad (8)$$

where $\langle . \rangle$ and $\sigma(\cdot)$ represent the mean and the standard deviation of the amino acids t^* in the analyzed protein.

Preliminary we analyzed which regions of proteins are in general characterized by small t^* and therefore key zone in the protein RINs. Intuitively, as shown in Figure 5 (see Appendix), surface charged residues and typical core residues are very fast in propagating the infection, because of the high energy interactions the charged residues are involved in and because of the high number of contacts the core residues have. Moreover, correlating secondary structure (as calculated by STRIDE [32]) of each residue with its t^* , we note that protein structured parts (Strand and AlphaHelix) are characterized by lower t^* , because when a residue is in an organized secondary structure, on average it is assembled in a dense part of the interaction network.

Since we are able to properly characterize the diffusive behavior at a single residue level, we investigated if amino acids that functionally need to have strong communication with the rest of the protein are characterized by peculiar diffusive properties. In this framework, one of the most important challenges in computational biology is the characterization of the active sites and allosteric domains in proteins, since the substrate binding in a distant site has to be detected through a cascade of residue-residue interactions [18].

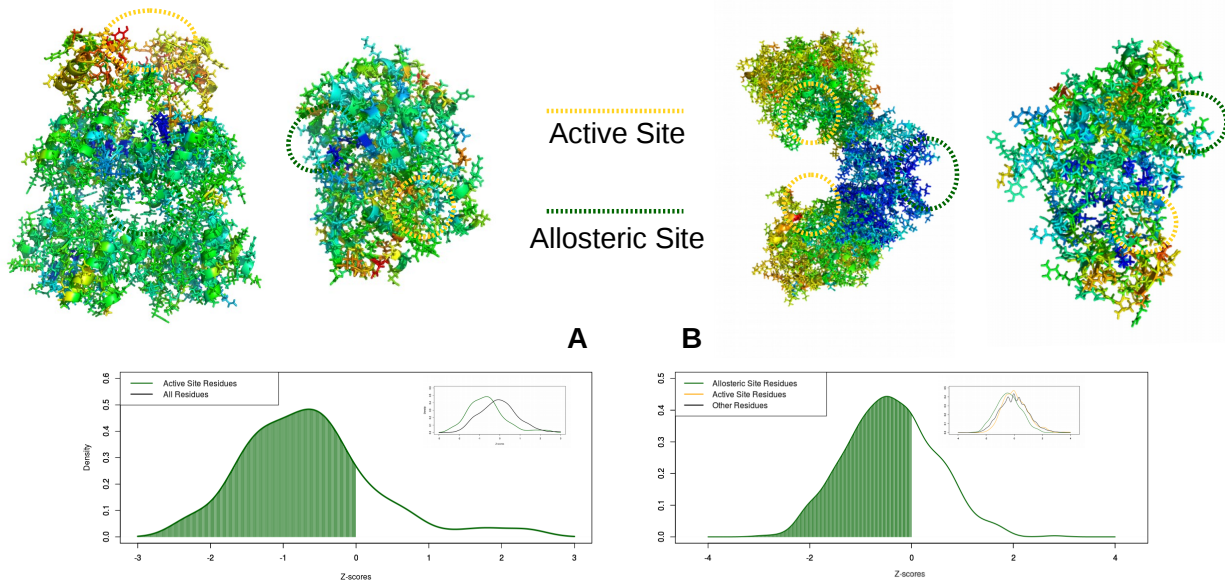


FIG. 3: Diffusive local characterization. Results are normalized over each protein in terms of z-scores calculated on the t_r as explained in formula 8. The molecular representation is obtained from 1D09, 1EFA, 1PTY, 2BRD and each amino acid is colored according to its t^* . **A)** Distribution of the z-score values regarding the active site amino acids of the 22 enzymes in the Tm dataset. **B)** Distribution of the z-score values regarding the active sites and allosteric sites amino acids of the 20 proteins in the allosteric dataset.

We proceeded to apply the diffusion protocol to the 11 pairs of (thermostable-mesostable) enzymes of the Enzyme dataset (for which we know the active site residues). The comparison between the diffusion of the active site residues and the other residues shows that typically the formers are characterized by a low t^* , since the information of binding needs to be fastly communicated to the whole protein. Indeed in Figure 3, the distribution of the z-scores belonging to the active site residues is shown. The 81% of them show a z-score lower than 0, meaning stronger connectivity with the whole protein than the average value of the other residues.

We now considered the 20 allosteric proteins with known active and allosteric site residues (see Allosteric dataset in Methods). As shown in Figure 3, the distribution of z-scores for the allosteric residues is statistically lower than 0, demonstrating that allosteric residues are faster than average in propagating information inside the protein network. The 73% of allosteric residues z-score distribution is lower than 0, and this peculiar diffusive behavior is due to their high functional role. Interestingly the active sites of these proteins are not characterized by peculiar diffusive characteristics (51% of the Z-score distribution is lower than 0). The cause of this behavior, different from what observed before, can be researched in the different binding state of the proteins: in the Tm dataset by construction the proteins are in the free form without ligands, while in the allosteric dataset the pro-

teins are prevalently in the bound form, with the ligand, occupying the active site.

F. HiV Proteases: a particular case of study

Finally, we turned to the HIV dataset and compared diffusion time Z-score associated with the residues of all the two variants of the HIV-protease. Each of the 18 protein can be represented with a diffusion time profile, which can be easily compared since all proteins have the same number of residues.

Figure 4a shows, as a heatmap, the result of a clustering analysis performed on residues and proteins of the dataset. All but one of the proteins are correctly identified as protease 1 or 2.

We then searched for the residues most responsible for the difference between the two protease sets. For each residue, we compared the distributions of the Z_i scores of HIV1 and HIV2 proteases. The 39 most different residues are 14, 19, 22, 23, 40, 41, 43, 56, 61, 62, 64, 70, 72, 73, 84, 95, 103, 108, 114, 115, 116, 118, 120, 134, 136, 140, 142, 155, 160, 163, 165, 167, 168, 170, 179, 190, 191, 192, 193, as discriminated by a p-value of 0.05. Notably, lowering the p-value threshold to 0.005, we identified a subgroup of seven residues, i.e. 14, 19, 64,95,118,142,190, shown in Figure 4b. Interestingly, those residues do not belong to the binding sites (see Figure 4c), suggesting a not trivial

action of distant mutations in modifying the affinity of the proteases to the drugs.

I. DISCUSSION

Usually, methods are very efficient in providing information about specific aspects of the inquired system, proteins though are complex system where evolution must be very proficient in tuning parameter (e.g. selecting mutations) to obtained more fitted proteins with respect to some features while maintaining functional proteins. For instance, optimizing enzymes to be more efficient at high temperature (i.e. increasing their thermal stability) must not reduce enzyme flexibility and ability to change configurations.

Graph theory-based method for the study of residue-residue interactions in the three-dimensional structure of proteins represents a powerful approach to investigate their topological and energetic properties. However, as is known, a static view of the protein structures does not allow us to describe their complexity in a complete way. To confirm this, several aspects of proteins were investigated through dynamical approaches, like molecular dynamics, perturbation-response approaches, which take into account the dynamical properties but typically are characterized by a high computational cost.

Here, we adopted an epidemic diffusion-based method which constitutes a compact way to study essential aspects of proteins, connected with their complex structural organization. The most striking advantage of this method is that it is not very computationally expensive allowing to explore complex problems like thermostability and information transfer. Starting from the RIN formalism [33, 34], we studied the diffusion of a fictitious epidemic inside the network using energies and node degrees as proxies of infection and recovery rates.

A large number of mathematical models have been formulated to study the spread of infectious diseases, but most of these are just variants of Kermack and McKendrick epidemic model [35, 36]. Reproducing different aspects of the spread of real diseases, all models ultimately provide a measure of the information diffusion throughout the entire network. Indeed, epidemic models indeed describe the dynamical evolution of the contagion process within a population.

Here we dealt with two crucial aspects related to the correct function of proteins. On the one hand, their ability to withstand the increase in temperature, i.e. their thermostability. On the other hand the property of rearranging the entire structure, or transmitting local conformational changes, due to the binding with other molecules. For this purpose, we have chosen to focus the diffusion analysis on active and allosteric sites.

Simulations of diffusion processes were performed considering typical network parameters for calculating the probability of transmission of infection (proportional to the link energy) and the probability of each node of re-

turning susceptible (proportional to node degree).

From diffusion simulations, two descriptors were defined, one (ρ^*) providing global information and the other (t^*) local one. In particular, a residue-specific descriptor is of fundamental importance because the identification of key residues in a protein structure is a useful tool for protein design in many open biological questions. A focus on the enzymes of the dataset was made in order to study the contribution of active site residues in relation to the rest of the structure in terms of epidemic spreading properties. The idea is that the infection initiated by the binding site residues spread sooner than other regions of the protein.

Considering the stationary phase, the mean of the percentage of infected nodes is constant over the steps balancing the rate of infection and recovery. The value of the stationary percentage of infected nodes is a very compact way to quantify global properties of the entire protein related to residue-residue energetic interactions. A protein characterized by strong interconnectivity will have a very strong energetic coupling between its residues showing, at the equilibrium, a higher number of infected nodes.

In the same way, it is necessary to take in account also the structural and geometrical characteristics, since strong energetic interactions, if not properly arranged, can cause local confinement of the epidemic without increasing the global number of infected nodes.

Given an overall fold, the arrangement of side chains organizes the inter-molecular interaction to better resist the thermal noise. Therefore, we test the sensibility of this formalism applying it on a well-defined set of homologous protein pairs, one from a mesostable organism and one from a thermostable one.

We find that proteins belonging to thermophilic organisms have a significantly higher percentage of infected residues than homologous mesophilic counterparts, meaning that thermophilic proteins organize their network of interactions in order to promote infection. We could, therefore, conclude that thermophilic proteins have, on average, a higher level of interconnectivity than mesophilic proteins.

Another important aspect dealt with in this work concerns the local properties of proteins that often present communication mechanisms even at long distances. In this case, the problem was studied by analyzing the transient phase of the diffusion simulation, that is composed of the steps between the initial infection and the reaching of the stationary state.

Starting from some nodes, the number of infected nodes changes rapidly to get to the equilibrium. The number of steps necessary in order to reach the stationary phase, t^* , is dependent on the choice of the starting nodes, expressing their centrality in the energy network. This local characterization can be utilized in order to identify which kind of residues (or domains) are more central in a protein, in terms of their connection with the rest of the protein.

In the analysis shown in this work, we find that both

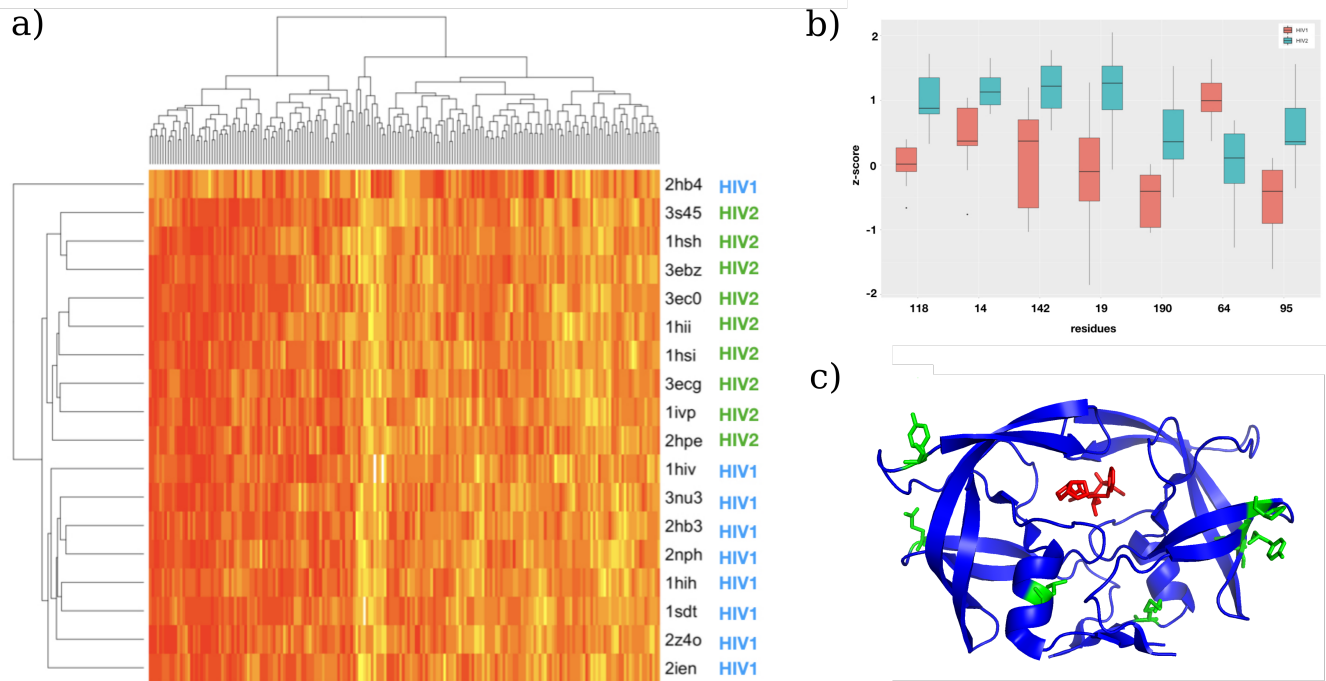


FIG. 4: **a)** Heatmap representation of the clustering analysis performed on the Z_i scores of the proteases of the HIV dataset. **b)** Boxplot of the distributions of the Z_i scores of the 7 most different HIV residues. **c)** Representation of the 3ECG HIV protease. Green sticks highlight the seven residues most responsible for the difference between HIV1 and HIV2 protease sets.

the residues belonging to the allosteric sites and those belonging to the active sites of enzymes, typically reach the state of equilibrium with a number of steps smaller than any other residue.

We also applied the local property of each residue to two sets of HIV variants. The method showed again its

ability to describe the complex system (protein) by analyzing the dynamic properties of its most elementary constituents (residues). Indeed, the analysis shows a clear division between the two groups of HIV variants in terms of transient phase analysis.

- [1] B. Chakrabarty and N. Parekh, *Nucleic Acids Research* **44**, W375 (2016).
- [2] N. V. Dokholyan, L. Li, F. Ding, and E. I. Shakhnovich, *Proceedings of the National Academy of Sciences* **99**, 8637 (2002).
- [3] A. del Sol, H. Fujihashi, D. Amoros, and R. Nussinov, *Molecular Systems Biology* **2** (2006).
- [4] G. Amitai, A. Shemesh, E. Sitbon, M. Shklar, D. Natanely, I. Venger, and S. Pietrokovski, *Journal of Molecular Biology* **344**, 1135 (2004).
- [5] M. Vendruscolo, N. V. Dokholyan, E. Paci, and M. Karplus, *Phys Rev E Stat Nonlin Soft Matter Phys* **65**, 061910 (2002).
- [6] M. Aftabuddin and S. Kundu, *Biophysical Journal* **93**, 225 (2007).
- [7] M. Miotto, P. P. Olimpieri, L. D. Rienzo, F. Ambrosetti, P. Corsi, R. Lepore, G. G. Tartaglia, and E. Milanetti, *Bioinformatics* (2018).
- [8] L.-Q. Yang, P. Sang, Y. Tao, Y.-X. Fu, K.-Q. Zhang, Y.-H. Xie, and S.-Q. Liu, *Journal of Biomolecular Structure and Dynamics* **32**, 372 (2013).
- [9] C. Castellano, S. Fortunato, and V. Loreto, *Reviews of Modern Physics* **81**, 591 (2009).
- [10] R. Albert and A.-L. Barabási, *Reviews of Modern Physics* **74**, 47 (2002).
- [11] K. V. Brinda and S. Vishveshwara, *Biophys. J.* **89**, 4159 (2005).
- [12] N. Kannan and S. Vishveshwara, *Protein Eng.* **13**, 753 (2000).
- [13] A. Mozo-Villarias, J. Cedano, and E. Querol, *Protein Engineering, Design and Selection* **16**, 279 (2003).
- [14] R. hard Sterner and W. Liebl, *Critical Reviews in Biochemistry and Molecular Biology* **36**, 39 (2001).
- [15] W. G. Touw, C. Baakman, J. Black, T. A. te Beek, E. Krieger, R. P. Joosten, and G. Vriend, *Nucleic Acids Res.* **43**, D364 (2015).
- [16] S. Pundir, M. J. Martin, and C. O'Donovan, *Methods Mol. Biol.* **1558**, 41 (2017).
- [17] R. Alcántara, J. Onwubiko, H. Cao, P. de Matos, J. A. Cham, J. Jacobsen, G. L. Holliday, J. D. Fischer, S. A. Rahman, B. Jassal, et al., *Nucleic Acids Research* **41**, D773 (2012).

- [18] B. R. C. Amor, M. T. Schaub, S. N. Yaliraki, and M. Barahona, *Nature Communications* **7** (2016).
- [19] D. Triki, T. Billot, B. Visseaux, D. Descamps, D. Flat- ters, A.-C. Camproux, and L. Regad, *Scientific reports* **8**, 5789 (2018).
- [20] J. C. Phillips, R. Braun, W. Wang, J. Gumbart, E. Tajkhorshid, E. Villa, C. Chipot, R. D. Skeel, L. Kale, and K. Schulten, *J Comput Chem* **26**, 1781 (2005).
- [21] K. Vanommeslaeghe and A. D. MacKerell, *J Chem Inf Model* **52**, 3144 (2012).
- [22] R. K. Grewal and S. Roy, *Protein Pept. Lett.* **22**, 923 (2015).
- [23] L. J. Allen, *Mathematical biosciences* **124**, 83 (1994).
- [24] R Core Team, *R: A Language and Environment for Sta- tistical Computing*, R Foundation for Statistical Comput- ing, Vienna, Austria (2013), ISBN 3-900051-07-0, URL <http://www.R-project.org/>.
- [25] A. Amadei, S. D. Galdo, and M. D’Abramo, *Journal of Biomolecular Structure and Dynamics* pp. 1–9 (2017).
- [26] G. G. Tartaglia, A. Cavalli, and M. Vendruscolo, *Struc- ture* **15**, 139 (2007).
- [27] S. Vishveshwara, K. V. Brinda, and N. Kannan, *Jour- nal of Theoretical and Computational Chemistry* **01**, 187 (2002).
- [28] M. Vijayabaskar and S. Vishveshwara, *Biophysical Jour- nal* **99**, 3704 (2010).
- [29] C. W. Lee, H. J. Wang, J. K. Hwang, and C. P. Tseng, *PLoS ONE* **9**, e112751 (2014).
- [30] B. Folch, Y. Dehouck, and M. Rooman, *Biophys. J.* **98**, 667 (2010).
- [31] B. Folch, M. Rooman, and Y. Dehouck, *J Chem Inf Model* **48**, 119 (2008).
- [32] D. Frishman and P. Argos, *Proteins: Structure, Func- tion, and Genetics* **23**, 566 (1995).
- [33] D. Sengupta and S. Kundu, *BMC Bioinformatics* **13** (2012).
- [34] C. Böde, I. A. Kovács, M. S. Szalay, R. Palotai, T. Kor- csmáros, and P. Csermely, *FEBS Letters* **581**, 2776 (2007).
- [35] W. O. Kermack and A. G. McKendrick, *Proceedings of the Royal Society A: Mathematical, Physical and Engi- neering Sciences* **115**, 700 (1927).
- [36] W. O. Kermack and A. G. McKendrick, *Proceedings of the Royal Society A: Mathematical, Physical and Engi- neering Sciences* **138**, 55 (1932).

| Couple | Thermostable | Mesostable | Active Site |
|--------|--------------|------------|--|
| 1 | 1FJQ | 1NPC | Tyr157; Asp226; His231; His142 A; His146 A; Glu 166 A; Glu 143 |
| 2 | 3PFK | 2PFK | Asp127; Gly 11; Arg72; Thr125; Arg171 |
| 3 | 1RIL | 2RN2 | Asp10; Asp70; Glu48; His124; Asp134 |
| 4 | 1BMD | 4MDH | His186; Asp158 |
| 5 | 2PRD | 1JFD | — |
| 6 | 1PHP | 3PGK | — |
| 7 | 1THM | 1ST3 | — |
| 8 | 1EBD | 1LVL | — |
| 9 | 1BTM | 1TIM | Gly171; Ser211; Lys13; Glu97; Asn11; His95; Glu165 |
| 10 | 1IQZ | 1DUR | — |
| 11 | 1VJW | 1FCA | — |
| 12 | 1XYZ | 2EXO | Glu127; Asp235; Asn169; Glu233; His205 |
| 13 | 1CAA | 1IRO | — |
| 14 | 2GD1 | 4GPD | — |
| 15 | 1TIB | 1LGY | — |
| 16 | 1ZIP | 2AKY | Lys1; Arg4 |
| 17 | 1AIS | 1VOL | — |
| 18 | 1FFH | 1FTS | — |
| 19 | 1OBR | 2CTC | His69; Glu72; His196; Arg127; Glu270 |
| 20 | 1PHN | 1CPC | — |
| 21 | 1BLI | 1HVX | — |
| 32 | 1TMY | 3CHY | — |
| 23 | 1AYG | 2PAC | — |
| 24 | 1GHS | 1GHR | Glu231; Glu279; Lys282; Glu288 |
| 25 | 1BVU | 1HRD | Asp165; Lys125 |
| 26 | 1CIU | 1CGT | — |
| 27 | 1OSI | 1CM7 | — |
| 28 | 3MDS | 1QNM | — |
| 29 | 1XGS | 1MAT | His161; Asp82; Asp93; His153; Glu187;Glu280; Glu187 |
| 30 | 1DL3 | 1PII | Cys7; Asp126 |
| 31 | 1IGS | 1PII | Asn180, Ser211; Glu51; Lys110; Glu159; Glu210; Lys53 |
| 32 | 1BXB | 1QT1 | — |

TABLE I: Table of the 32 couples of proteins of the T_m dataset, collected from the literature. The proteins corresponding to the rows of the table with the annotated active site are enzymes and constitute the "Enzyme Dataset".

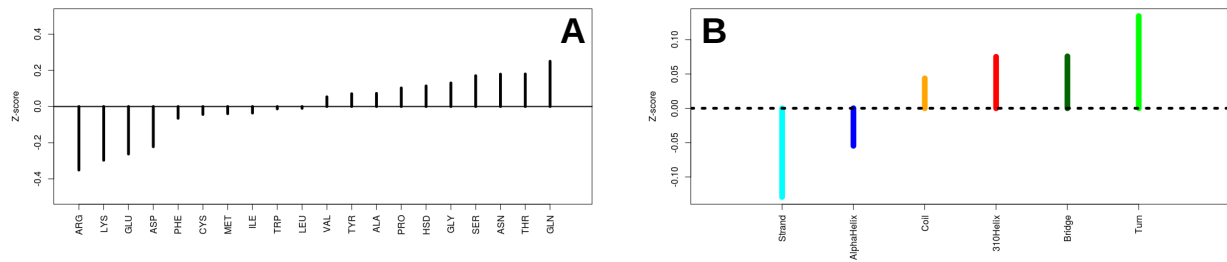


FIG. 5: **A)** The mean t_r for each of the 20 amino acids in all proteins of thermostable dataset. **B)** B The mean t_r for each type of secondary structure, obtained using all proteins of thermostable dataset.